

## REVIEW

## Recent progress in poly(ethylene oxide)-based solid-state electrolytes for lithium-ion batteries

Jiyoung Lee  | Byeong-Su Kim Department of Chemistry, Yonsei University,  
Seoul, Republic of Korea

## Correspondence

Byeong-Su Kim, Department of Chemistry,  
Yonsei University, Seoul 03722, Republic of  
Korea.Email: [bskim19@yonsei.ac.kr](mailto:bskim19@yonsei.ac.kr)

## Funding information

National Research Foundation of Korea,  
Grant/Award Numbers: NRF-  
2018R1A5A1025208, NRF-2021R1A2C3004978

## Abstract

In this review, we discuss the latest research trends related to poly(ethylene oxide) (PEO)-based solid-state polymer electrolytes for application in lithium-ion batteries. First, the characteristics of PEO-based polymer electrolytes, highlighted as the next-generation electrolytes for batteries, are briefly introduced. Next, based on the findings reported in the recent literature, strategies to address their inherent challenges, such as low-ionic conductivity at room temperature, concentration polarization, and poor mechanical properties, are covered. Finally, their remaining challenges and future prospects are outlined.

## KEYWORDS

lithium-ion batteries, organic–inorganic hybrids, PEO-based polymer electrolytes, single-ion conducting electrolytes, solid-phase electrolytes

## INTRODUCTION

Due to their excellent charge and discharge performance and low self-discharge rate, lithium-ion batteries (LIBs) are in widespread use as the primary energy source for myriad electronic devices, as well as electric vehicles.<sup>1–4</sup> To date, most of electrolytes that mediate the movement of lithium cations in LIBs are liquids consisting of lithium salts such as lithium bis(trifluoromethanesulfonyl)imide (LiTFSI) dissolved in organic carbonate solvents.<sup>5</sup> However, they are known to pose serious safety issues due to their high volatility, flammability, and potential for leakage.<sup>6–9</sup> Moreover, if the temperature of the battery cell rises unexpectedly due to an internal short circuit caused by an external impact, the battery can easily explode or ignite.<sup>10</sup> In addition, a liquid electrolyte can contribute to the growth of lithium dendrites on the surface of the anode, which can lead to an internal short circuit between the electrodes that causes the separator to be penetrated, resulting in an explosion and/or fire within the cell.<sup>11</sup> Therefore, to address these challenges, a diverse range of research has been conducted toward replacing conventional liquid electrolytes with solid-state ones.<sup>12</sup>

Solid-phase electrolytes mainly include both inorganic and polymer electrolytes, with the latter having relatively better interfacial contact with the electrodes as well as

higher flexibility.<sup>13</sup> The most widely studied polymer electrolytes are based on PEO with good solvation capacity for lithium cations, which is advantageous for lithium cation transport.<sup>14</sup> PEO can interact with lithium cations by coordinating four or five ether oxygen atoms with a lithium cation (Figure 1a).<sup>15</sup> The transport of lithium cations occurs through the breaking/formation of lithium-oxygen bonds.<sup>19</sup> However, since PEO is semi-crystalline at room temperature (Figure 1b),<sup>16</sup> continuous segmental rearrangement becomes difficult in the crystalline region, which hinders the transport of lithium cations. As such, PEO-based polymers exhibit low conductivity at room temperature.<sup>16,20</sup> In this context, strategies such as polymer blending and copolymer formation have been reported to improve ionic conductivity by suppressing the crystallinity of PEO.

On the other hand, polymer electrolytes composed of lithium salts and a polymer matrix can facilitate the migration of both lithium cations and counteranions in opposite directions during charge and discharge cycles, referred to as a dual-ion conductor. However, lithium cations typically exhibit lower mobility compared to their counteranions because of their strong coupling with Lewis basic sites within the polymeric matrix.<sup>17,21</sup> As a result, severe concentration gradients of lithium cation can interfere with the uniform deposition of lithium cations on the anode, leading to the nucleation of

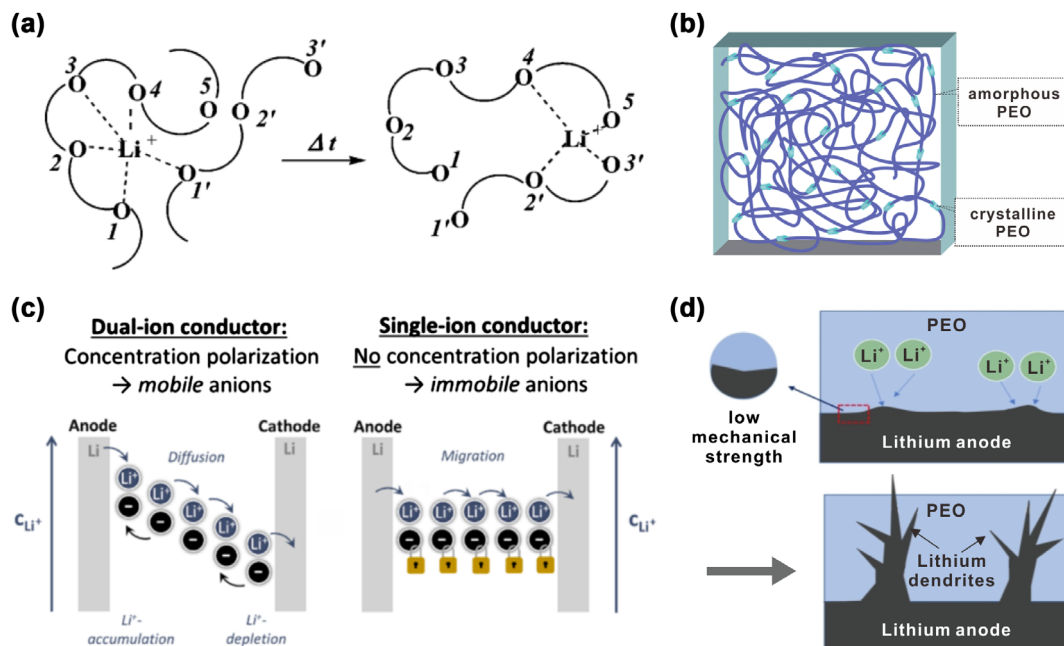


**FIGURE 1** Lithium-ion transport properties of poly(ethylene oxide) (PEO)-based polymer electrolytes with challenges. (a) The lithium-ion transport mechanism of PEO. Reprinted with permission from Xu,<sup>15</sup> Copyright 2004, American Chemical Society. (b) The semi-crystalline morphology of PEO. Reproduced with permission from Xue et al.,<sup>16</sup> Copyright 2015, The Royal Society of Chemistry. (c) Comparison of the single-ion conduction system with dual-ion system. Reprinted with permission from Stolz et al.,<sup>17</sup> Copyright 2022, American Chemical Society. (d) The lithium dendrite growth mechanisms of PEO. Reproduced with permission from Zhang et al.,<sup>18</sup> Copyright 2022, Elsevier.

lithium dendrites.<sup>22–24</sup> Therefore, the concept of a single-ion conductor, which is designed to immobilize the counteranion while allowing only the lithium cation to move, has attracted significant attention. Single-ion conducting polymer electrolytes can be used to immobilize anions and achieve a lithium-ion transference number near unity (Figure 1c).<sup>17</sup> Immobilizing anions can be achieved by anchoring anions through covalent bonds to polymer chains or by capturing anions through anion receptors.<sup>25</sup>

Although the flexibility of polymer electrolytes is favorable for lithium-ion transport, there is the problem of the formation of lithium dendrites that can penetrate the electrode (Figure 1d).<sup>18,26</sup> In addition, since the electrodes of LIBs undergo intercalation and de-intercalation processes involving lithium cations during charging and discharging, respectively, the polymer electrolyte must possess sufficient mechanical strength to withstand the accompanying volume changes of the electrodes.<sup>19</sup> Therefore, strategies such as introducing crosslinking to enhance the mechanical strength of PEO or modifying PEO to confer the self-healing property so that the LIB can recover readily from an external impact have been reported.

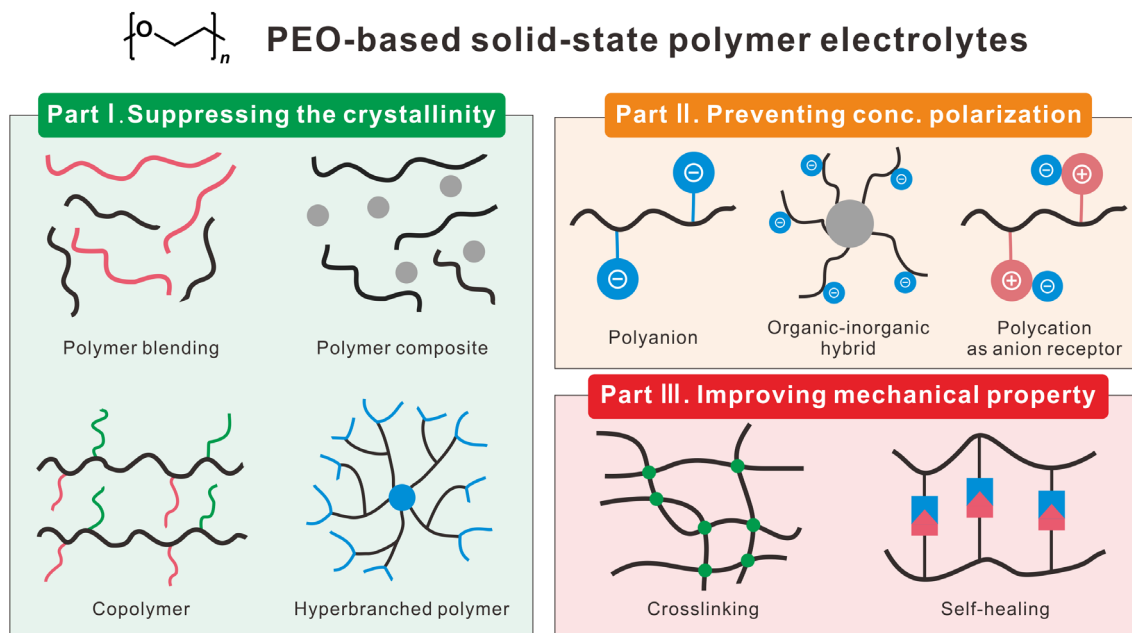
In this review, we discuss the solid-state PEO-based electrolytes, particularly from the collection of recent literatures with a focus on the strategies for their improvement in the following main categories (Scheme 1): (1) strategies to inhibit crystallinity, (2) strategies to

prevent concentration polarization, and (3) strategies to improve mechanical properties. The specific approaches reported for each objective are highlighted with representative examples.

## Strategies for suppressing the crystallinity of PEO-based polymer electrolytes

### Polymer blending

Polymer blending offers a straightforward and effective approach for increasing the amorphous regions in PEO-based polymers that enables the properties to be readily controlled by altering the composition.<sup>27,28</sup> For example, Pol et al. reported a composite electrolyte consisting of poly(tetrafluoroethylene) (PTFE)-blended PEO (Figure 2a).<sup>29</sup> The fluorine atom in PTFE is capable of forming a hydrogen bond with the hydroxyl group of PEO, leading to disordering of the crystal structure of PEO. By incorporating PTFE, the ionic conductivity of the composite at room temperature ( $6.62 \times 10^{-8}$  S/cm) was increased by three times compared to PEO ( $2.25 \times 10^{-8}$  S/cm), accompanied by improvements in the capacity and cycling stability at the same time. Moreover, the high melting point of PTFE ( $T_m = 326^\circ\text{C}$ ) effectively improved the thermal stability of the composite electrolyte at high temperatures.



**SCHEME 1** Strategies for improving poly(ethylene oxide) (PEO)-based solid-state polymer electrolytes for use in LIBs: (1) suppressing their crystallinity, (2) preventing concentration polarization, and (3) improving their mechanical properties.

## Polymer composites with inorganic materials

The incorporation of inorganic materials with high ionic conductivity into polymer electrolytes has been widely studied as a simple and practical approach for improving the latter.<sup>33</sup> The resulting composite polymer electrolyte often more closely meets the performance requirements for LIBs.<sup>34–36</sup> Toward this end, Zhou's group applied an  $\text{Li}_{6.4}\text{La}_3\text{Zr}_{1.4}\text{Ta}_{0.6}\text{O}_{12}$  (LLZTO) filler (Figure 2b).<sup>30</sup> Specifically, a PEO-based composite electrolyte was designed by adding LLZTO filler and succinonitrile (SN) plasticizer to PEO, from which an electrolyte film was produced using polyacrylonitrile (PAN) as a support. The Lewis acid–base interaction between LLZTO and TFSI<sup>−</sup> and the interaction between SN and lithium cations prevented the crystallization of PEO and immobilized the anions, which improved the solubility and transport of lithium salts. In addition, the chemical interaction between PAN and LLZTO generated a local conjugated structure, which enabled the transfer of lithium cations to the interface between LLZTO and PAN. The composite electrolyte film demonstrated an electrochemical stability window of 4.7 V, ionic conductivity of  $2.57 \times 10^{-4}$  S/cm at 30°C, and a lithium-ion transference number of 0.6.

Sun et al. applied aluminum-based metal–organic framework (MOF) nanorods as an inorganic filler,<sup>37</sup> which effectively hindered the crystallinity of PEO by reducing the interactions between the PEO chains. In addition, the microporous and micrometer-length MOF nanorods favored the transport of lithium cations more than bulky TFSI<sup>−</sup> anions, thus enabling fast lithium-ion transport. Therefore, PEO-MOF5% polymer electrolytes containing

5% MOF nanorods improved the electrochemical properties of PEO significantly, including improved ionic conductivity ( $2.09 \times 10^{-5}$  S/cm at 30°C and  $7.11 \times 10^{-4}$  S/cm at 60°C), an expanded electrochemical window of 4.7 V, and a higher lithium-ion transference number of 0.46. In addition, an all-solid-state LIB containing PEO-MOF5% displayed a high capacity of 167.3 mAh/g and a capacity retention rate of 87.1% after 100 cycles.

## Block copolymers

The synthesis of block copolymer electrolyte has been suggested as an effective method for optimizing the properties of a polymer electrolyte. Block copolymers consist of covalently bonded blocks of polymers that enable the realization of unique properties based on those of the single polymer systems therein.<sup>38,39</sup>

As a representative example, Xue's group prepared block copolymers via a single-step method by combining reversible addition-fragmentation chain transfer polymerization and carboxylic acid-catalyzed ring-opening polymerization (ROP) (Figure 2c).<sup>31</sup> The design of the block copolymer was aimed at enhancing the migration of lithium cations in the polyether-based polymer by introducing polyester matrixes that provide relatively weak coordination with the cations. In addition, the carboxylic acid group can simultaneously play the role of catalyzing ROP and stabilizing the interface. The assembled Li/LFP (lithium ferrous phosphate) battery with the copolymer retained 92% of its capacity at a rate of 1 C after 400 cycles.

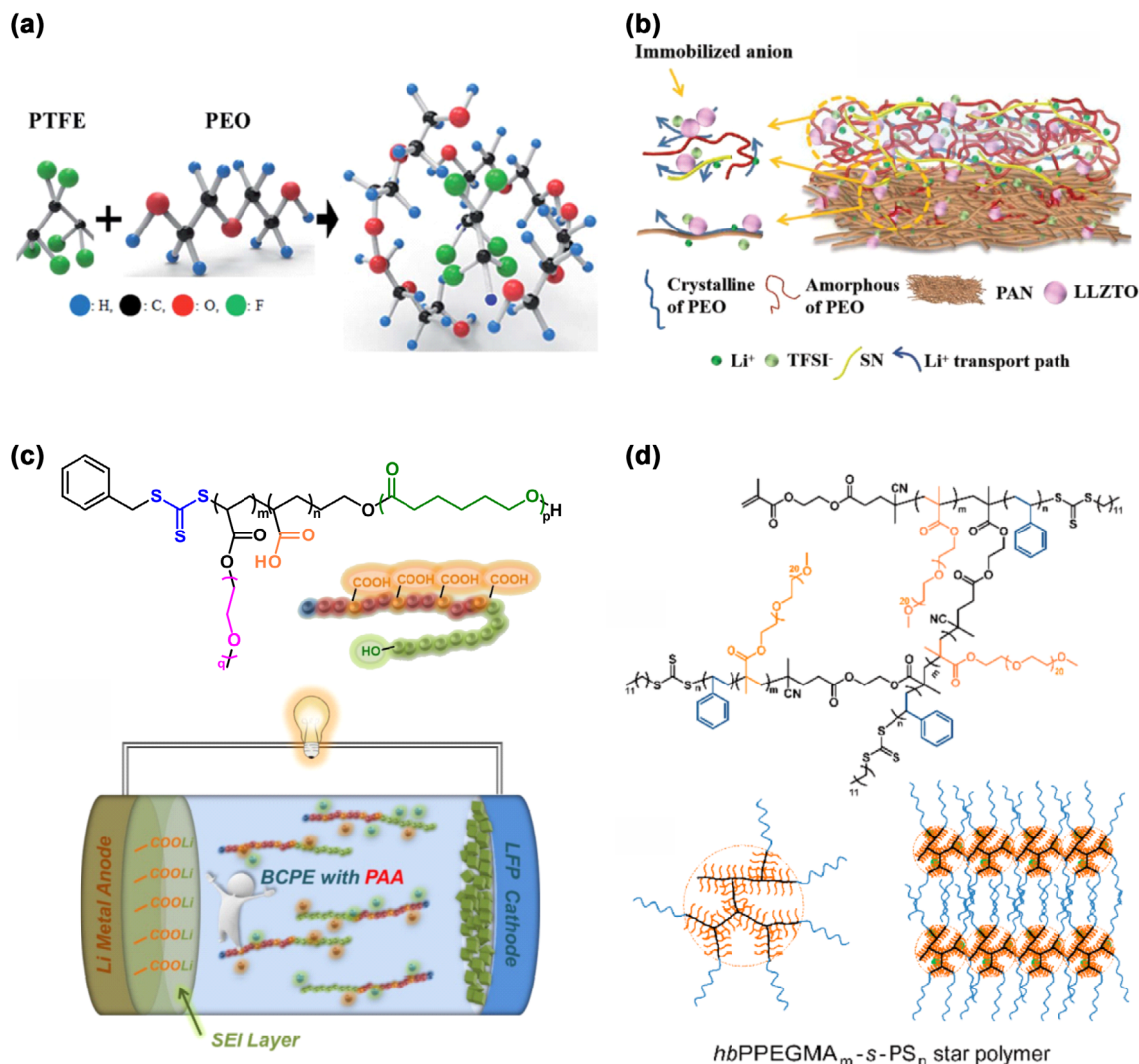


**FIGURE 2** (a) The blending of poly(tetrafluoroethylene) (PTFE)-PEO composite electrolytes causing disorder of the crystalline structure of PEO. Reprinted with permission from Jokhakar et al.,<sup>29</sup> Copyright 2020, Royal Society of Chemistry. (b) The enhanced ionic conduction of a PEO-based composite electrolyte via blending with inorganic filler  $\text{Li}_{6.4}\text{La}_3\text{Zr}_{1.4}\text{Ta}_{0.6}\text{O}_{12}$  (LLZTO) and plasticizer succinonitrile (SN). Reprinted with permission from Gao et al.,<sup>30</sup> Copyright 2022, John Wiley & Sons, Inc. (c) The block copolymer consisted of brush-like poly(poly(ethylene glycol) methyl ether acrylate) (PPEGA) block for restraining the crystallinity of PEO, polyacrylic acid (PAA) block for suppressing the side reaction of the electrolyte and poly( $\epsilon$ -caprolactone) (PCL) block for facilitating the transference of lithium-ion. Reprinted with permission from Guo et al.,<sup>31</sup> Copyright 2023, John Wiley & Sons, Inc. (d) The hyperbranched structure of poly(poly(ethylene glycol) methyl ether methacrylate)-*star*-polystyrene ( $\text{hbPPEGMA}_m\text{-s-PS}_n$ ) star polymer for inhibiting crystallization and promoting PEO segmental motion. Reprinted with permission from Chen et al.<sup>32</sup> Copyright 2019, American Chemical Society.

In another noteworthy effort, Nealey and coworkers conducted a detailed analysis that revealed differences in the ion conduction mechanisms of electrolytes comprising polystyrene-*block*-poly(ethylene oxide) (SEO)-LiTFSI block copolymer electrolyte or PEO-LiTFSI.<sup>40</sup> They found that SEO-LiTFSI and PEO-LiTFSI exhibited the highest ionic conductivity when the lithium/ethylene oxide (Li/EO) ratio was 1/12. However, when the Li/EO ratio exceeded 1/12, the conductivity of PEO-LiTFSI decreased while that of SEO-LiTFSI remained constant. This is because, in the case of SEO-LiTFSI, the excess lithium cations tended to coordinate with the counteranions more effectively than with the EO units. This phenomenon

enabled the excess lithium salt to be separated from the polymeric domain, thereby preventing inhibition of the segmental dynamics.

### Hyperbranched polymer electrolytes

A hyperbranched polymer is a type of dendritic polymer that has a spherical core structure with several flexible polymer branches. The hyperbranched structure incorporating short chains is capable of dissociating lithium salts onto the backbone, which prevents the regular alignment of the PEO chains. Therefore, it effectively promotes the

**TABLE 1** Representative examples of PEO-based electrolytes produced via strategies for suppressing crystallinity.

Entry	Type	Polymer structure	Coulombic efficiency	$T_g$ (°C)	$\sigma$ (S/cm)	Ref.
1	Polymer blending	PEO/PTFE/LiTFSI	99.9% after 50 cycles at 0.5 C	–	$6.62 \times 10^{-8}$ at 30°C	29
2	Polymer blending	PEO/PLiMTFSI	–	–	$2.1 \times 10^{-4}$ at 70°C	43
3	Polymer composite	PEO-60LLZTO-SN	97.6% after 100 cycles at 0.2 C	–55.25	$2.57 \times 10^{-4}$ at 30°C	30
4	Polymer composite	PEO-MOF5%	99% after 100 cycles at 0.1 C	–	$7.11 \times 10^{-4}$ at 60°C	37
5	Copolymer	P(AA-co-PEGMA)- <i>b</i> -PCL	99% after 180 cycles at 0.1 C	–36.34	$3.14 \times 10^{-5}$ at ~25°C	31
6	Copolymer	SEO-LiTFSI	–	–	$\sim 10^{-3}$ at 100°C	40
7	Hyperbranching	<i>hb</i> PPEGMA <sub><i>m</i></sub> - <i>s</i> -PS <sub><i>n</i></sub>	99% after 100 cycles at 0.2 C	–47, 101	$9.5 \times 10^{-5}$ at 60°C	32

Abbreviations: AA, acrylic acid; *hb*PPEGMA<sub>*m*</sub>-*s*-PS<sub>*n*</sub>, poly(poly(ethylene glycol) methyl ether methacrylate)-*star*-polystyrene; LiTFSI, lithium bis(trifluoromethanesulfonyl)imide; MOF, metal-organic framework; PCL, poly( $\epsilon$ -caprolactone); PEGMA, poly(ethylene glycol) methyl ether acrylate; PEO, poly(ethylene oxide); PLiM TFSI, poly(lithium 1-[3-(methacryloyloxy) propylsulfonyl]-1-(trifluoromethanesulfonyl) imide); PTFE, poly(tetrafluoroethylene); SEO, polystyrene-*block*-poly(ethylene oxide);  $T_g$ , glass transition temperature;  $\sigma$ , ionic conductivity.

ionic stability of PEO-based electrolytes (even at room temperature) by reducing the crystallinity of PEO.<sup>41,42</sup> According to the study by Yao and coworkers, a hyperstar solid polymer electrolyte such *hb*PPEGMA<sub>*m*</sub>-*s*-PS<sub>*n*</sub> can improve lithium-ion transport by inhibiting the crystallization of the PEO domain (Figure 2d).<sup>32</sup> Moreover, it enhances the mechanical properties by efficiently entangling the linear PS arm. The hyperstar polymers exhibited an ionic conductivity of  $9.5 \times 10^{-5}$  S/cm and a storage modulus of 0.5 MPa at 60°C. Furthermore, when applied to a Li/LiFePO<sub>4</sub> battery, it provided an excellent capacity of 142 mAh/g after 100 cycles at 0.2 C (see representative examples summarized in Table 1).

## Strategies for preventing concentration polarization of PEO-based polymer electrolytes

### Polyanion in polymer backbone

The simplest way to obtain a single-ion conducting polymer electrolyte is by attaching anionic functional groups to the polymer backbone through covalent bonds. For example, this can be achieved by polymerizing the anionic components of a lithium salt or incorporating them into the polymer backbone via post-polymerization. However, achieving high ionic conductivity can be challenging when the lithium cations are strongly bound to their counteranions. Therefore, anionic moieties that are large with a delocalized charge, such as sulfonate and sulfonylimide, are typically used for this purpose.<sup>44</sup> Recently, novel strategies that extend beyond simply linking anionic groups to the polymer backbone, such as introducing anionic groups into flexible polyether blocks<sup>45,46</sup> or blending with PEO,<sup>43,47</sup> to enhance other properties that affect lithium-ion transport such as the segmental dynamics of the polymer have been reported.

Frey et al. produced a single-ion conducting polymer electrolyte called PEO-*b*-(EO-co-lithium trifluoromethanesulfonamide)ethyl glycidyl ether (LiTFSAEGE) by covalently grafting TFSI<sup>–</sup> anions into a polystyrene (PS)-*b*-PEO

block copolymer (Figure 3a).<sup>48</sup> TFSI<sup>–</sup> anionic groups are often located in the PS block in conventional PS-*b*-PEO copolymer-based single-ion conducting polymers. However, in this study, TFSI<sup>–</sup> anionic groups were successfully introduced into the flexible PEO block to reduce PEO-induced crystallinity and immobilize the anionic group. PEO-*b*-(EO-co-LiTFSAEGE) exhibited ionic conductivity of  $\sim 10^{-6}$  S/cm at 400 K, which is approximately two orders of magnitude improvement compared to that of PS-*b*-PEO/lithium triflate (LiTf). Moreover, PEO-*b*-(EO-co-LiTFSAEGE) exhibited a lithium-ion conductivity similar to PEO-*b*-PSLiTFSI while maintaining an ordered morphology and mechanical stability at high temperature.

Winey's group fabricated single-ion conducting polymer blend electrolytes composed of a polymer functionalized with TFSI<sup>–</sup> on every fifth carbon in the PS backbone (p5PhTFSI-Li) and PEO.<sup>46</sup> The single-ion conducting polymer not only prevented concentration polarization by anchoring the TFSI<sup>–</sup> counteranion group to the polystyrene backbone but also the swelling of polar aggregates upon blending with PEO. Moreover, the interaction between the lithium cations and PEO weakened the interaction between lithium cations and TFSI<sup>–</sup>. Consequently, when the operating temperature exceeded the glass transition temperature (i.e.,  $T \gg T_g$ ), a superionic transport mechanism was observed where the ionic conductivity was decoupled from the segmental motion of PEO due to the competition between two transport mechanisms: one involving the hopping of lithium cations between TFSI<sup>–</sup> anions and the other via coupling with segmental relaxation. Furthermore, the parallel study mentioned that p5PhTFSI-Li blended with PEO demonstrated high lithium-ion transference number of approximately unity.<sup>50</sup> In particular, the ionic conductivity was greater than  $10^{-5}$  and  $10^{-4}$  S/cm at 90°C and 130°C, respectively, with high PEO content (an EO-to-Li<sup>+</sup> ratio of 10).

### Organic-inorganic hybrids

Ionic functional groups can be incorporated into an organic/inorganic hybrid by functionalizing inorganic

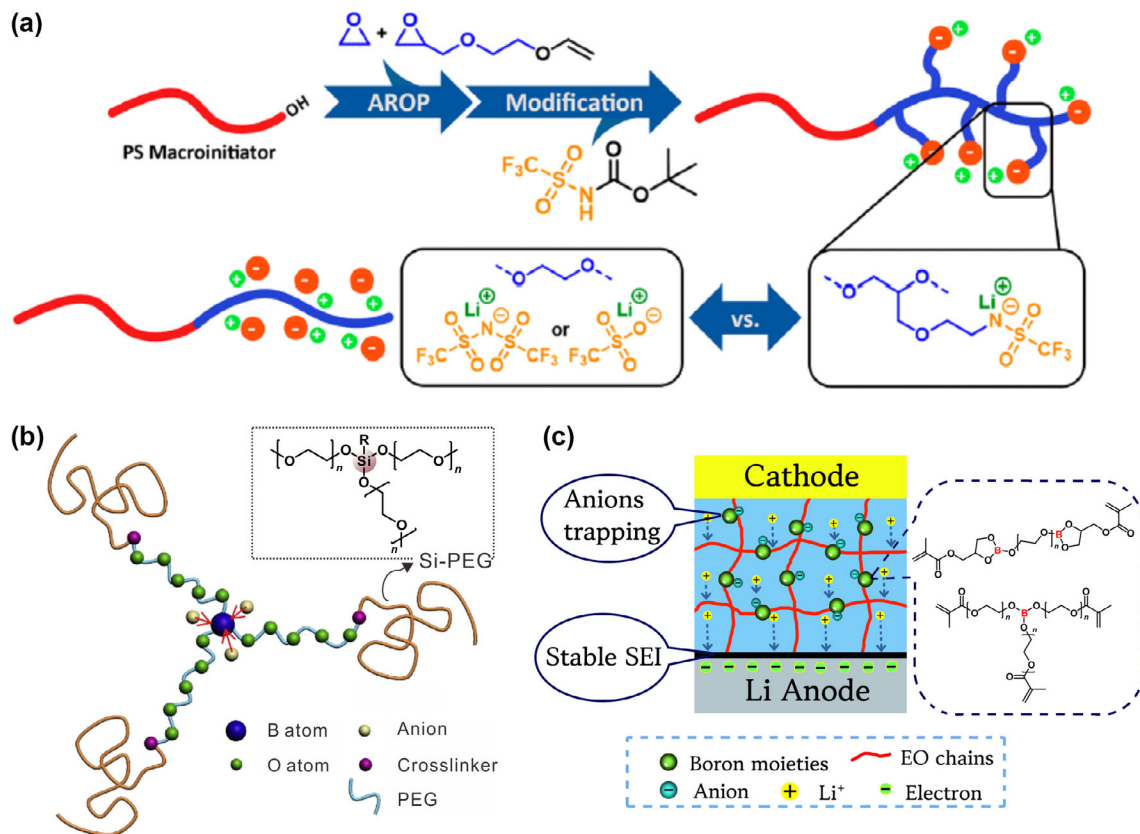


**FIGURE 3** Schematic diagrams of (a) covalent attachment of TFSI<sup>-</sup> anion into the polyether block of the polystyrene (PS)-*b*-P(ethylene oxide) (EO)-*co*-(lithium trifluoromethanesulfonamide)ethyl glycidyl ether (LiTFSAEGE). Reprinted with permission from Dreier et al.,<sup>48</sup> Copyright 2022, American Chemical Society. (b) The single-ion conducting property from the Lewis acidity of boron of the hybrid solid polymer electrolyte. Reprinted with permission from Li et al.,<sup>49</sup> Copyright 2019, Elsevier. (c) A borate-rich gel polymer electrolyte with a 3D crosslinked structure (3D-BGPE) with anion immobilizing boron moieties. Reprinted with permission from Dai et al.,<sup>25</sup> Copyright 2019, Royal Society of Chemistry.

nanoparticles with ion conducting moieties. For example, Shi et al. reported a hybrid solid polymer electrolyte in which borate ester-polyethylene glycol (B-PEG) was covalently attached to a silicon-doped polyethylene glycol (Si-PEG) network (Figure 3b).<sup>49</sup> Boron plays a critical role in attracting anions of lithium salts to reduce concentration polarization, and the Lewis acidity of boron is less shielded by the connected PEG chains, which effectively improves lithium-ion transfer. In addition, the presence of a flexible Si–O–C chain in the main chain resulted in high ionic conductivity of  $1.6 \times 10^{-4}$  S/cm at 25°C and a high lithium-ion transference number of 0.68. Furthermore, when applied in a Li/LFP cell, the capacity retention reached 84% after 100 cycles at 25°C at a rate of 1 C (see representative examples summarized in Table 2).

In another example, Sun et al. produced an anion-immobilized composite electrolyte (P@CMOF) consisted of cationic MOF (CMOF) and PEO/LiTFSI matrix.<sup>52</sup> The CMOF can immobilize anions through electrostatic interactions. Furthermore, the –NH<sub>2</sub> group of CMOF can protect the ether oxygen of the PEO chains via hydrogen bonding, increasing the electrochemical stability. The polymer electrolyte exhibited excellent electrochemical performance, including superb ionic conductivity of  $6.3 \times 10^{-4}$  S/cm at 60°C, enlarged electrochemical

window of 4.97 V, and a high lithium-ion transference number of 0.72. Moreover, the Li/LiFePO<sub>4</sub> cell with this electrolyte maintained a capacity retention of 85.4% after 300 cycles at 60°C and a current density of 1 C.

### Polymers with anion receptor groups

Incorporating anion receptors into single-ion conducting polymers is a viable approach to enhance the lithium-ion transference number. The principle of immobilizing the counteranion in this strategy relies on a Lewis acid–base interaction, where the anion receptor serves as a Lewis acid (electron pair acceptor) and the counteranion acts as a Lewis base (electron pair donor). Typically, these anion receptors are organoboron compounds, known for their strong electron-accepting properties, enabling effective interaction with the counteranion.<sup>21,54</sup> For instance, Wei et al. prepared a borate-rich gel polymer electrolyte with a 3D crosslinked structure (3D-BGPE) that contained a Lewis acid boron ester via in situ polymerization of a mixture of linear boron-containing crosslinker (LBC), branched boron-containing crosslinker (TBC), and 1 M LiTFSI/ethylene carbonate (EC)/dimethyl carbonate (DMC) (Figure 3c).<sup>25</sup> Their density functional theory calculations revealed that

**TABLE 2** Representative examples of PEO-based electrolytes via strategies for preventing concentration polarization.

Entry	Type	Polymer structure	Coulombic efficiency	$t_+$	$\sigma$ (S/cm)	Ref.
1	Polyanion	PEO- <i>b</i> -(EO- <i>co</i> -LiTFSAEGE)	–	–	$10^{-6}$	48
2	Polyanion	Polymer blend of p5PhTFSI-Li and PEO	–	$\sim 1$	$>10^{-5}$ at 90 °C	46
3	Polyanion	$sp^3$ boron atom-based single-ion-conducting polymer	–	0.88	$1.46 \times 10^{-5}$ at 60 °C	51
4	Organic-inorganic hybrid	Crosslinked Si-PEG network with B-PEG	–	0.68	$1.6 \times 10^{-4}$ at 25 °C	49
5	Organic-inorganic hybrid	Polymer electrolyte with a CMOF	(Initial) 94.1% at 0.1 C	0.72	$6.3 \times 10^{-4}$ at 60 °C	52
6	Polymer with anion receptor group	3D-BGPE	89.73% after 400 cycles at 0.5 C	0.76	$8.4 \times 10^{-4}$ at 30 °C	25
7	Polymer with anion receptor group	Crosslinked polymer electrolyte network with a boronic ester	99% after 500 cycles at 1 C	0.79	$2.52 \times 10^{-3}$ at 25 °C	53

Abbreviations: 3D-BGPE, a borate-rich gel polymer electrolyte with a 3D crosslinked structure; EO, ethylene oxide; LiTFSAEGE, (lithium trifluoromethanesulfonamide)ethyl glycidyl ether; P@CMOF, anion-immobilized composite electrolyte consisted of cationic metal-organic framework (MOF); p5PhTFSI, a bis(trifluoromethanesulfonyl)imide ion (TFSI<sup>-</sup>) on every fifth carbon in the polystyrene backbone; PEO, poly(ethylene oxide);  $t_+$ , lithium-ion transference number;  $\sigma$ , ionic conductivity.

the interaction energies of TFSI<sup>-</sup> for boron atoms in TBC and LBC were  $-45.76$  and  $-29.08$  kJ/mol, respectively, confirming that TFSI<sup>-</sup> could be successfully immobilized by the interaction between boron and TFSI<sup>-</sup>. 3D-BGPE exhibited a high lithium-ion transference number of 0.76, excellent ionic conductivity of  $8.4 \times 10^{-4}$  S/cm, and a wide electrochemical stability window of up to 4.52 V. In addition, the Li/LFP cell with 3D-BGPE showed a high-capacity retention rate of 89.7% even after 400 cycles at 0.5 C and 30 °C.

Meng et al. used Lewis acid allylboronic acid pinacol ester groups as anion receptors to capture bis(fluorosulfonyl) imide (FSI) and difluoro(oxalato)borate (DFOB) anions.<sup>53</sup> The resulting polymer exhibited high ionic conductivity of  $2.52 \times 10^{-3}$  S/cm at 25 °C and a high lithium-ion transference number of 0.79 while also demonstrating an excellent rate capacity (a specific capacity of 112.4 mAh/g at 5 C) and long-term cycling stability (93.2% capacity retention after 500 cycles) when applied to Li/LFP cells.

## Strategies for improving the mechanical properties of PEO-based polymer electrolytes

### Crosslinking the polymer electrolytes

Crosslinking induced by either light or heat is a commonly used strategy to enhance the mechanical strength of PEO-based electrolytes.<sup>55</sup> As a representative example, Zhou et al. produced a PEO-polyacrylonitrile (PAN) copolymer (Figure 4a),<sup>56</sup> with PAN acting as both a filler and crosslinker to improve the mechanical strength and ionic conductivity of the electrolyte. PEO-PAN-LiTFSI demonstrated outstanding mechanical strength by withstanding a weight of 200 g and remained stable under tensile stress of 2.0 MPa. Moreover, it exhibited a 10-fold enhancement in ionic conductivity at room temperature with reduced crystallinity compared to PEO-LiTFSI. Furthermore, the  $-C=N-O$  functional group of PEO-PAN-LiTFSI strongly adsorbs

polysulfides, thereby suppressing shuttling and enhancing the rate performance and cycling stability of lithium-sulfur batteries. Last, the capacity retention rate was over 96% after 1000 bending cycles.

In another example, Gerbaldi et al. produced a UV-crosslinked polymer electrolyte comprising PEO, tetra(ethylene glycol)dimethyl ether, and LiTFSI (Figure 4b).<sup>57</sup> The UV-crosslinked polymer electrolyte displayed superior mechanical properties at high temperatures, with a higher storage modulus ( $G'$ ) value than its viscous modulus ( $G''$ ) value between 20 °C and 130 °C. In addition, UV-induced crosslinking reduced the crystallinity of the polymer matrix and decreased ionic aggregation, leading to remarkable electrochemical properties including an improved lithium-ion transference number above 0.5 and ionic conductivity over  $1 \times 10^{-4}$  S/cm at ambient temperature.

### Self-healing polymer electrolytes

LIBs are subjected to localized stresses due to strain during operation, which can lead to catastrophic cracking. Continual accumulation of stress can damage the battery, and the presence of cracks can promote the growth of lithium dendrites and irregular lithium deposition. Therefore, imparting self-healing properties that can readily recover from external damage has emerged as a useful approach for improving the mechanical properties of polymer electrolytes.<sup>60,61</sup>

In this context, Xue et al. imparted disulfide bonds to a PEO-based polymer electrolyte via the radical photopolymerization of an S-S crosslinker and PEG methyl ether acrylate (Figure 4c).<sup>58</sup> The resulting polymer exhibited the self-healing property, which was attributed to dynamic disulfide and hydrogen bonds. After 2 h at 80 °C, the truncated polymer electrolyte was completely recovered. Furthermore, the active chain segment transfer resulting from disulfide metathesis led to an improvement in ionic conductivity at room temperature of  $1.24 \times 10^{-4}$  S/cm.

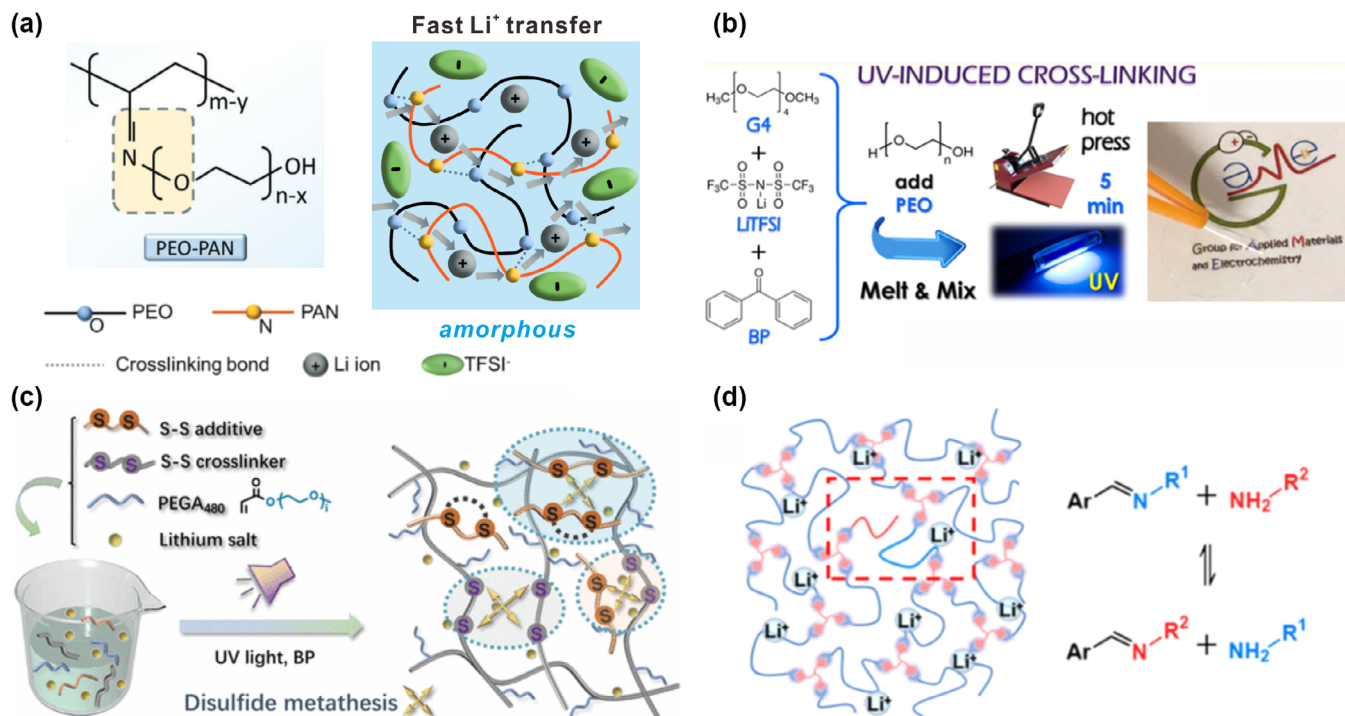


**FIGURE 4** (a) Schematic illustration of crosslinking mechanism and improved lithium-ion transfer of PEO–polyacrylonitrile (PAN). Reprinted with permission from Sheng et al.,<sup>56</sup> Copyright 2022, John Wiley & Sons, Inc. (b) The preparation of a UV-crosslinked polymer electrolyte. Reprinted with permission from Falco et al.,<sup>57</sup> Copyright 2019, American Chemical Society. (c) The disulfide metathesis-assisted lithium-ion conduction of self-healable polymer electrolyte. Reprinted with permission from Wang et al.,<sup>58</sup> Copyright 2022, American Chemical Society. (d) The self-healing mechanism of polymer electrolyte bearing dynamic imine bonds. Reprinted with permission from Zhange et al.,<sup>59</sup> Copyright 2021, American Chemical Society.

**TABLE 3** Representative examples of PEO-based electrolytes via strategies for improving the mechanical properties.

Entry	Type	Polymer structure	Coulombic efficiency	Tensile strength (MPa)	$\sigma$ (S/cm)	Ref.
1	Crosslinking	PEO–PAN–LiTFSI	99% after 50 cycles at 0.1 C	>2.0	$1.63 \times 10^{-5}$ at ambient temperature	56
2	Crosslinking	UV-crosslinked polymer based on PEO, tetra(ethylene glycol)dimethyl ether and LiTFSI	99% after 400 cycles at 1 C	–	$>1 \times 10^{-4}$ at ambient temperature	57
3	Crosslinking	Dual-salt PEO-based polymer electrolyte	99% after 100 cycles at 0.1 C	1.75	$5.7 \times 10^{-4}$ at 30°C	62
4	Self-healing polymer electrolyte	Disulfide bond-based network polymer	99.7% after 100 cycles at 0.1 C	–	$1.24 \times 10^{-4}$ at 30°C	58
5	Self-healing polymer electrolyte	Imine bond-based network polymer	99% after 300 cycles at 0.1 C	0.137	$7.48 \times 10^{-4}$ at 25°C	59
6	Self-healing polymer electrolyte	Disulfide bond-based network polymer	–	–	$1 \times 10^{-4}$ at 90°C	63
7	Self-healing polymer electrolyte	Disulfide bond and hydrogen bond-based network polymer	99.8% after 100 cycles at 0.1 C	–	$7.28 \times 10^{-6}$ at 30°C	64

Abbreviations: LiTFSI, lithium bis(trifluoromethanesulfonyl)imide; PAN, polyacrylonitrile; PEO, poly(ethylene oxide);  $\sigma$ , ionic conductivity.

On the other hand, Pu et al. reported PEO-based self-healing polymer electrolyte bearing dynamically crosslinked imine bonds (Figure 4d).<sup>59</sup> Dynamic covalent polymer networks based on reversible covalent bonds could spontaneously restore their structure and function without any

external stimuli. The incorporation of imine conferred excellent mechanical properties (extensibility >500% and stress >130 kPa), reduced the crystallinity of the polymer electrolyte, significantly improved ionic conductivity to  $7.48 \times 10^{-4}$  S/cm at 25°C, and provided strong adhesion, thus



favoring effective contact between the electrolyte and the electrode. The polymer electrolyte also exhibited a wide electrochemical window and a tensile strain of 524%. As a result, when applied to an Li/LFP cell, it maintained a discharge capacity of 126.4 mAh/g at 27°C after 300 cycles at a rate of 0.1 C (see representative examples summarized in Table 3).

## SUMMARY AND OUTLOOK

In this review, we presented the latest trends in the development of PEO-based solid-state polymer electrolytes. Various strategies for overcoming the inherent challenges of PEO-based polymer electrolytes, such as low-ionic conductivity at room temperature, concentration polarization, and poor mechanical stiffness, were discussed. These strategies involve modifying PEO-based polymer electrolytes by introducing various functional groups or structures to impart diverse properties. Nonetheless, PEO-based polymer electrolytes still face certain challenges that need to be addressed. First, there is a trade-off relationship between the ionic conductivity and mechanical strength of polymer electrolytes. The segmental motion is closely linked to ionic conductivity, making it difficult to achieve both sufficient ionic conductivity and desirable mechanical properties simultaneously.<sup>65,66</sup> Second, particularly in composite electrolytes, the inadequate interfacial contact between the electrode and electrolyte results in the degradation of high-energy density and long-term stability.<sup>67,68</sup> Finally, development of reprocessable and recyclable polymer electrolytes is crucial to deal with environmental issues.<sup>69</sup> Therefore, further research efforts are desirable to overcome these challenges. In this regard, we propose the following three strategies: (1) The incorporation of crystalline lithium cation conducting pathway to decouple segmental motion and ionic conductivity. This can be achieved through the alignment of polymer chains via supramolecular self-assembly.<sup>70</sup> For example, zwitterionic polymer electrolytes with bulky charges immobilized on the polymer backbone can be utilized to ensure sufficient free volume for the transport of lithium cations.<sup>71</sup> (2) The synthesis of polymer electrolytes through in situ polymerization using UV irradiation or thermocuring, which reduces interfacial resistance between the electrode and electrolyte. Polymerizable monomers in the liquid phase can be wetted onto the electrode and polymerized on the electrode surface, forming a stable interface.<sup>72,73</sup> Crosslinked polymer electrolytes can also provide mechanical stability, and the use of a porous supporting skeleton can maintain stability without compromising ionic conductivity.<sup>74</sup> (3) The preparation of polymer electrolytes with dynamic bonds through chemical crosslinking, allowing recyclability and reprocessability. Vitrimer-based polymer electrolytes with dynamic covalent bonds, such as boronic ester bonds, exhibit excellent mechanical properties similar to thermosetting polymers at room temperature, as well as ductility and reprocessability

at high temperatures.<sup>69,75</sup> These strategies are anticipated to improve the properties of PEO-based solid-state electrolytes, making them promising alternative for developing high-performance lithium battery electrolytes in the future.

## ACKNOWLEDGMENTS

This work was supported by the National Research Foundation of Korea (NRF-2021R1A2C3004978 and NRF-2018R1A5A1025208).

## ORCID

Jiyoung Lee  <https://orcid.org/0000-0002-6009-7524>

Byeong-Su Kim  <https://orcid.org/0000-0002-6419-3054>

## REFERENCES

- [1] G. Jeong, Y.-U. Kim, H. Kim, Y.-J. Kim, H.-J. Sohn, *Energy Environ. Sci.* **2011**, *4*, 1986.
- [2] M. Lee, J. Jung, Y.-K. Han, *Bull. Korean Chem. Soc.* **2018**, *39*, 1227.
- [3] J.-G. Han, E. Hwang, Y. Kim, S. Park, K. Kim, D.-H. Roh, M. Gu, S.-H. Lee, T.-H. Kwon, Y. Kim, N.-S. Choi, B.-S. Kim, *ACS Appl. Mater. Interfaces* **2020**, *12*, 24479.
- [4] M. Gu, S. Ko, S. Yoo, E. Lee, S. H. Min, S. Park, B.-S. Kim, *J. Power Sources* **2015**, *300*, 351.
- [5] P. K. Sahu, J. Kim, K. Park, E. Kim, S. Mondal, K. Kwak, M. Cho, *Bull. Korean Chem. Soc.* **2022**, *43*, 215.
- [6] B. Scrosati, J. Garche, *J. Power Sources* **2010**, *195*, 2419.
- [7] X. Feng, M. Ouyang, X. Liu, L. Lu, Y. Xia, X. He, *Energy Storage Mater.* **2018**, *10*, 246.
- [8] G. J. Chung, J. Han, S.-W. Song, *ACS Appl. Mater. Interfaces* **2020**, *12*, 42868.
- [9] J.-A. Choi, E.-G. Shim, D.-W. Kim, *Bull. Korean Chem. Soc.* **2010**, *31*, 3190.
- [10] Q. Wang, P. Ping, X. Zhao, G. Chu, J. Sun, C. Chen, *J. Power Sources* **2012**, *208*, 210.
- [11] D. Hong, Y. Choi, J. Ryu, J. Mun, W. Choi, M. Park, Y. Lee, N.-S. Choi, G. Lee, B.-S. Kim, S. Park, *J. Mater. Chem. A* **2019**, *7*, 20325.
- [12] C.-H. Doh, Y.-C. Ha, Y.-J. Lee, J.-H. Yu, *Bull. Korean Chem. Soc.* **2018**, *39*, 1149.
- [13] A. Arya, A. L. Sharma, *Ionics* **2017**, *23*, 497.
- [14] L. Long, S. Wang, M. Xiao, Y. Meng, *J. Mater. Chem. A* **2016**, *4*, 10038.
- [15] K. Xu, *Chem. Rev.* **2004**, *104*, 4303.
- [16] Z. Xue, D. He, X. Xie, *J. Mater. Chem. A* **2015**, *3*, 19218.
- [17] L. Stolz, S. Hochstädt, S. Röser, M. R. Hansen, M. Winter, J. Kasnatscheew, *ACS Appl. Mater. Interfaces* **2022**, *14*, 11559.
- [18] Q. Zhang, B. Yue, C. Shao, H. Shao, L. Li, X. Dong, J. Wang, W. Yu, *Chem. Eng. J.* **2022**, *443*, 136479.
- [19] D. Zhou, D. Shanmukaraj, A. Tkacheva, M. Armand, G. Wang, *Chem* **2019**, *5*, 2326.
- [20] I. Shin, K. Lee, E. Kim, T.-H. Kim, *Bull. Korean Chem. Soc.* **2018**, *39*, 1058.
- [21] H. Zhang, C. Li, M. Piszcz, E. Coya, T. Rojo, L. M. Rodriguez-Martinez, M. Armand, Z. Zhou, *Chem. Soc. Rev.* **2017**, *46*, 797.
- [22] J. Zhu, Z. Zhang, S. Zhao, A. S. Westover, I. Belharouak, P.-F. Cao, *Adv. Energy Mater.* **2021**, *11*, 2003836.
- [23] J. Shim, H. J. Kim, B. G. Kim, Y. S. Kim, D.-G. Kim, J.-C. Lee, *Energy Environ. Sci.* **2017**, *10*, 1911.
- [24] K. Deng, D. Han, S. Ren, S. Wang, M. Xiao, Y. Meng, *J. Mater. Chem. A* **2019**, *7*, 13113.
- [25] K. Dai, C. Ma, Y. Feng, L. Zhou, G. Kuang, Y. Zhang, Y. Lai, X. Cui, W. Wei, *J. Mater. Chem. A* **2019**, *7*, 18547.
- [26] D. Cao, X. Sun, Q. Li, A. Natan, P. Xiang, H. Zhu, *Matter* **2020**, *3*, 57.
- [27] S. K. Patla, R. Ray, K. Asokan, S. Karmakar, *J. Appl. Phys.* **2018**, *123*, 125102.
- [28] L. Zhu, J. Li, Y. Jia, P. Zhu, M. Jing, S. Yao, X. Shen, S. Li, F. Tu, *Int. J. Energy Res.* **2020**, *44*, 10168.

- [29] D. A. Jokhakar, D. Puthusseri, P. Manikandan, Z. Li, J. Moon, H.-J. Weng, V. G. Pol, *Sustain. Energy Fuels* **2020**, *4*, 2229.
- [30] L. Gao, B. Tang, H. Jiang, Z. Xie, J. Wei, Z. Zhou, *Adv. Sustain. Syst.* **2022**, *6*, 2100389.
- [31] K. Guo, J. Wang, Z. Shi, Y. Wang, X. Xie, Z. Xue, *Angew. Chem., Int. Ed.* **2023**, *62*, e202213606.
- [32] Y. Chen, Y. Shi, Y. Liang, H. Dong, F. Hao, A. Wang, Y. Zhu, X. Cui, Y. Yao, *ACS Appl. Energy Mater.* **2019**, *2*, 1608.
- [33] J. S. Kim, J. K. Lim, J. S. Park, *Bull. Korean Chem. Soc.* **2019**, *40*, 898.
- [34] L. Yang, Z. Wang, Y. Feng, R. Tan, Y. Zuo, R. Gao, Y. Zhao, L. Han, Z. Wang, F. Pan, *Adv. Energy Mater.* **2017**, *7*, 1701437.
- [35] Y. Zhao, Z. Huang, S. Chen, B. Chen, J. Yang, Q. Zhang, F. Ding, Y. Chen, X. Xu, *Solid State Ionics* **2016**, *295*, 65.
- [36] A. ElBellhi Abdelhameed, A. Bayoumy Wafaa, M. Masoud Emad, A. Mousa Mahmoud, *Bull. Korean Chem. Soc.* **2012**, *33*, 2949.
- [37] Z. Zhang, J.-H. You, S.-J. Zhang, C.-W. Wang, Y. Zhou, J.-T. Li, L. Huang, S.-G. Sun, *ChemElectroChem* **2020**, *7*, 1125.
- [38] Z. Ye, Z.-K. Zhang, S.-P. Ding, D.-L. Xia, J.-T. Xu, *ACS Appl. Polym. Mater.* **2023**, *5*, 120.
- [39] D. Devaux, D. Glé, T. N. T. Phan, D. Gignes, E. Giroud, M. Deschamps, R. Denoyel, R. Bouchet, *Chem. Mater.* **2015**, *27*, 4682.
- [40] D. Sharon, P. Bennington, M. A. Webb, C. Deng, J. J. de Pablo, S. N. Patel, P. F. Nealey, *J. Am. Chem. Soc.* **2021**, *143*, 3180.
- [41] G. Chen, L. Ye, K. Zhang, M. Gao, H. Lu, H. Xu, Y. Bai, C. Wu, *Chem. Eng. J.* **2020**, *394*, 124885.
- [42] J. Wang, S. Li, Q. Zhao, C. Song, Z. Xue, *Adv. Funct. Mater.* **2021**, *31*, 2008208.
- [43] J. L. Olmedo-Martínez, L. Porcarelli, Á. Alegría, D. Mecerreyes, A. J. Müller, *Macromolecules* **2020**, *53*, 4442.
- [44] J. Gao, C. Wang, D.-W. Han, D.-M. Shin, *Chem. Sci.* **2021**, *12*, 13248.
- [45] Y. Cai, C. Liu, Z. Yu, H. Wu, Y. Wang, W. Ma, Q. Zhang, X. Jia, *J. Power Sources* **2022**, *537*, 231478.
- [46] B. A. Paren, N. Nguyen, V. Ballance, D. T. Hallinan, J. G. Kennemur, K. I. Winey, *Macromolecules* **2022**, *55*, 4692.
- [47] J. L. Olmedo-Martínez, L. Porcarelli, G. Guzmán-González, I. Calafel, M. Forsyth, D. Mecerreyes, A. J. Müller, *ACS Appl. Polym. Mater.* **2021**, *3*, 6326.
- [48] P. Dreier, A. Pipertzis, M. Spyridakou, R. Mathes, G. Floudas, H. Frey, *Macromolecules* **2022**, *55*, 1342.
- [49] D. Li, X. Ji, X. Gong, F. Tsai, Q. Zhang, L. Yao, T. Jiang, R. K. Y. Li, H. Shi, S. Luan, D. Shi, *J. Power Sources* **2019**, *423*, 349.
- [50] N. Nguyen, M. P. Blatt, K. Kim, D. T. Hallinan, J. G. Kennemur, *Polym. Chem.* **2022**, *13*, 4309.
- [51] G. Guzmán-González, H. J. Ávila-Paredes, E. Rivera, I. González, *ACS Appl. Mater. Interfaces* **2018**, *10*, 30247.
- [52] H. Huo, B. Wu, T. Zhang, X. Zheng, L. Ge, T. Xu, X. Guo, X. Sun, *Energy Storage Mater.* **2019**, *18*, 59.
- [53] K. Deng, T. Guan, F. Liang, X. Zheng, Q. Zeng, Z. Liu, G. Wang, Z. Qiu, Y. Zhang, M. Xiao, Y. Meng, L. Wei, *J. Mater. Chem. A* **2021**, *9*, 7692.
- [54] K. Deng, Q. Zeng, D. Wang, Z. Liu, Z. Qiu, Y. Zhang, M. Xiao, Y. Meng, *J. Mater. Chem. A* **2020**, *8*, 1557.
- [55] M. L. Lehmann, G. Yang, D. Gilmer, K. S. Han, E. C. Self, R. E. Ruther, S. Ge, B. Li, V. Murugesan, A. P. Sokolov, F. M. Delnick, J. Nanda, T. Saito, *Energy Storage Mater.* **2019**, *21*, 85.
- [56] J. Sheng, Q. Zhang, C. Sun, J. Wang, X. Zhong, B. Chen, C. Li, R. Gao, Z. Han, G. Zhou, *Adv. Funct. Mater.* **2022**, *32*, 2203272.
- [57] M. Falco, C. Simari, C. Ferrara, J. R. Nair, G. Meligrana, F. Bella, I. Nicotera, P. Mustarelli, M. Winter, C. Gerbaldi, *Langmuir* **2019**, *35*, 8210.
- [58] H. Wang, Y. Huang, Z. Shi, X. Zhou, Z. Xue, *ACS Macro Lett.* **2022**, *11*, 991.
- [59] L. Zhang, P. Zhang, C. Chang, W. Guo, Z. H. Guo, X. Pu, *ACS Appl. Mater. Interfaces* **2021**, *13*, 46794.
- [60] M. J. Webber, M. W. Tibbitt, *Nat. Rev. Mater.* **2022**, *7*, 541.
- [61] T. Ye, L. Li, Y. Zhang, *Adv. Funct. Mater.* **2020**, *30*, 2000077.
- [62] F. Fu, Y. Zheng, N. Jiang, Y. Liu, C. Sun, A. Zhang, H. Teng, L. Sun, H. Xie, *Chem. Eng. J.* **2022**, *450*, 137776.
- [63] R. Kato, P. Mirmira, A. Sookezian, G. L. Grocke, S. N. Patel, S. J. Rowan, *ACS Macro Lett.* **2020**, *9*, 500.
- [64] Y. H. Jo, S. Li, C. Zuo, Y. Zhang, H. Gan, S. Li, L. Yu, D. He, X. Xie, Z. Xue, *Macromolecules* **2020**, *53*, 1024.
- [65] N. A. Stolwijk, M. Wiencierz, C. Heddiar, J. Kösters, *J. Phys. Chem. B* **2012**, *116*, 3065.
- [66] E. Glynos, P. Petropoulou, E. Mygiakis, A. D. Nega, W. Pan, L. Papoutsakis, E. P. Giannelis, G. Sakellariou, S. H. Anastasiadis, *Macromolecules* **2018**, *51*, 2542.
- [67] J. Pan, P. Zhao, N. Wang, F. Huang, S. Dou, *Energy Environ. Sci.* **2022**, *15*, 2753.
- [68] R. Rojaee, S. Cavallo, S. Mogurampelly, B. K. Wheatle, V. Yurkiv, R. Deivanayagam, T. Foroosan, M. G. Rasul, S. Sharifi-Asl, A. H. Phakatkar, M. Cheng, S.-B. Son, Y. Pan, F. Mashayek, V. Ganesan, R. Shahbazian-Yassar, *Adv. Funct. Mater.* **2020**, *30*, 1910749.
- [69] Y. Lin, Y. Chen, Z. Yu, Z. Huang, J.-C. Lai, J. B. H. Tok, Y. Cui, Z. Bao, *Chem. Mater.* **2022**, *34*, 2393.
- [70] D. Bresser, S. Lyonard, C. Iojoiu, L. Picard, S. Passerini, *Mol. Syst. Des. Eng.* **2019**, *4*, 779.
- [71] S. D. Jones, H. Nguyen, P. M. Richardson, Y.-Q. Chen, K. E. Wyckoff, C. J. Hawker, R. J. Clément, G. H. Fredrickson, R. A. Segalman, *ACS Cent. Sci.* **2022**, *8*, 169.
- [72] S.-K. Cho, H.-I. Kim, J.-W. An, K. Jung, H. Bae, J. H. Kim, T. Yim, S.-Y. Lee, *Adv. Funct. Mater.* **2020**, *30*, 2000792.
- [73] Z. Wang, L. Shen, S. Deng, P. Cui, X. Yao, *Adv. Mater.* **2021**, *33*, 2100353.
- [74] Z. Wang, Q. Guo, R. Jiang, S. Deng, J. Ma, P. Cui, X. Yao, *Chem. Eng. J.* **2022**, *435*, 135106.
- [75] W. Gu, F. Li, T. Liu, S. Gong, Q. Gao, J. Li, Z. Fang, *Adv. Sci.* **2022**, *9*, 2103623.

## AUTHOR BIOGRAPHIES

**Jiyoung Lee** is currently a PhD student in Prof. Byeong-Su Kim's group in the Department of Chemistry at Yonsei University. She received her BS and MS from the Department of Chemistry at Soongsil University, Republic of Korea, in 2018 and 2020. Her research interests include nanomaterials and polymers for energy conversion.

**Byeong-Su Kim** is an Underwood Distinguished Professor in the Department of Chemistry at Yonsei University, Republic of Korea. He received his BS and MS in Chemistry from Seoul National University and his PhD in Chemistry from the University of Minnesota, Twin Cities, in 2007. After his postdoctoral research at MIT, he started his independent career at UNIST in 2009 and moved to Yonsei University in 2018. His research group investigates a broad range of topics in macromolecular chemistry to study novel polymer and hybrid nanomaterials, including the molecular design and synthesis of self-assembled polymers and hybrid nanostructures.

**How to cite this article:** J. Lee, B.-S. Kim, *Bull. Korean Chem. Soc.* **2023**, *44*(10), 831. <https://doi.org/10.1002/bkcs.12767>